Influence of Solution Treatment on the Adsorption and Morphology of Poly(*o*-methoxyaniline) Layer-by-Layer Films

Nara C. de Souza,[†] Josmary R. Silva,[‡] Renato Di Thommazo,[§] Maria Raposo,[||] Débora T. Balogh,[§] José A. Giacometti,[†] and Osvaldo N. Oliveira, Jr.*[,§]

Faculdade de Ciências e Tecnologia, Universidade Estadual Paulista, CP 467, 19060-900 Presidente Prudente, SP, Brazil, Instituto de Física, Universidade Federal de Goiás, CP 131, 74001-970 Goiânia, Go, Brazil, Instituto de Física de São Carlos, Universidade de São Paulo, CP 369, 13560-970 São Carlos, SP, Brazil, and Faculdade de Ciência e Tecnologia, Universidade Nova de Lisboa, 2815-114 Monte Caparica, Portugal

Received: December 15, 2003; In Final Form: July 5, 2004

It is shown that the adsorption and morphological properties of layer-by-layer films of poly(*o*-methoxyaniline) (POMA) alternated with poly(vinyl sulfonic acid) (PVS) are affected dramatically by different treatments of the POMA solutions employed to prepare the films. Whereas the dimension of the globular structures seen by atomic force microscopy increases nonmonotonically during film growth in parent POMA solution, owing to a competition of adsorption/desorption processes, it changes monotonically for the fractionated POMA. The roughness of the latter films depends on the concentration of the solution and saturates at a given size of the scan window. This allowed us to apply scaling laws that indicated a self-affine mechanism for adsorption of the treated POMA.

I. Introduction

The growth of molecularly flat, highly uniform thin films is required for a number of sophisticated devices employing molecular electronics principles. The layer-by-layer (LBL) or self-assembly technique[1] has held great promise because it can lead to supramolecular structures similar to those built with the Langmuir−Blodgett (LB) technique,[2] with the advantage of requiring much simpler experimental procedures. Multilayer films can have a much greater roughness than expected for LBL films, primarily because of aggregation in polymers that are prone to H-bonding in addition to electrostatic attractions.[3] Control of the structure of such films is possible only if the factors affecting morphology and growth mechanisms are known in great detail. In this context, the kinetics of the processes involved in the adsorption of LBL films are still a matter of debate.[4] LBL films resulting from physical adsorption have been classified[5] according to the adsorption mechanisms as follows: (i) LBL films from highly charged, strong polyelectrolytes are molecularly thin with adsorption governed almost entirely by ionic interactions. (ii) For LBL films from partially charged, weak polyelectrolytes, the thickness can vary by 1 order of magnitude,[6] depending on the pH of the polymer solutions. (iii) The third group comprises films in which secondary interactions such as H-bonding play a prominent role in adsorption. In some cases, H-bonding can even be the primary mechanism for film formation. The thicknesses of such films can vary widely, from molecularly thin to very thick layers, including cases of non-self-limited adsorption.[3] (iv) The final class consists of LBL films adsorbed via special interactions, such as the biotin−avidin attraction.[7]

LBL films from polyaniline and its derivatives have been studied extensively,[8−18] but there are still several open points, particularly because H-bonding plays a prominent role in the formation of these films. Here, we show that the methods used to treat poly(*o*-methoxyaniline) (POMA) solutions can affect the adsorption as well as the morphology of LBL films of POMA alternated with poly(vinylsulfonic acid) (PVS). The films were analyzed using UV−vis spectroscopy, atomic force microscopy, and scanning electron microscopy.

II. Experimental Details

POMA was synthesized according to the route described by Mattoso et al.[19] and used in the doped state (emeraldine salt). POMA solutions were prepared as follows: For solution 1, 1.202 g of POMA was swollen in 20 mL of acetonitrile, which was then diluted with 980 mL of ultrapure water supplied by a Milli-Q system. The mixture was subjected to magnetic stirring for 4 h, allowed to rest for 2 h, and was then filtered with a ceramic filter with 25−50-μm pores. The filtrate (solution 1) pH was adjusted to 3 by the addition of appropriate amounts of a 1 M HCl aqueous solution. Solution 1 had a concentration of 0.6 g/L and could be diluted by addition of water, yielding solution 1* with a concentration of 0.03 g/L. The final concentrations of all POMA solutions employed in this work were determined by UV−vis measurements using dilute solutions of POMA with known concentrations for calibration. Both solutions 1 and 1* were used for producing LBL films. The molecular weight distribution of POMA was obtained for the undoped sample state in a system similar to that used by Mattoso

* To whom correspondence should be addressed. Tel: + 55-16 273-9825. Fax: + 55 16 271-5365. E-mail: chu@if.sc.usp.br.
[†] Universidade Estadual Paulista.
[‡] Universidade Federal de Goiás.
[§] Universidade de São Paulo.
[||] Universidade Nova de Lisboa.

10.1021/jp037873a CCC: $27.50
Published on Web 08/14/2004

et al.[19] The undoped sample was prepared by evaporating 100 mL of solution 1 to dryness and dedoping it with ammonium hydroxide. The dark blue powder was completely dissolved in *N*-methyl-2-pyrrolidone (NMP, 2.5 mg/mL). This solution was subjected to size-exclusion chromatography (SEC) analysis in a Shimadzu chromatographic system with a refraction index detector, using two PLgel-mixed-C columns, NMP (0.7 mL/min) as the solvent at 60 °C, and polystyrene standards. As shown later in this work, POMA from solution 1 is highly polydisperse. Attempts were made to fractionate it by various methods, such as solution fractionation of the undoped POMA, but they were all unsuccessful. The application of more time-consuming methods of fractionation, such as gel filtration and other more expensive chromatographic methods, is now under investigation. In these attempts, we observed that, upon addition of 1 M HCl to solution 1 under magnetic stirring, a partial precipitation occurred. The precipitate was colloidal and could not be recovered by either filtration or centrifugation. Nevertheless, applying the procedure to a POMA solution in which the step using acetonitrile was skipped resulted in a precipitate that could be easily separated. In this procedure, solution 2 was prepared adding 1.202 g of POMA (emeraldine salt) to 1 L of water, with the following steps identical to those employed for solution 1. That is, stirring, filtering, and adjustment of the pH were carried out as in solution 1, followed by the addition of 1 M HCl until precipitation. Two different fractions could be separated by the stepwise addition of HCl to solution 2, after the solution had been allowed to rest for 2 h and then filtered twice. The more soluble fraction that passed through the filter (filtrate) was tested directly in the LBL process. The amount of material adsorbed in the LBL process with this fraction was 10 times less than that for other solutions, and therefore it was not used in further experiments. The POMA precipitated (left in the filter) was then used to prepare a solution using the same procedure as used for solution 2, which is hereafter referred to as solution 3. Solution 3 had a concentration of 0.03 g/L and a pH of 3 and was used to produce LBL films. An attempt to increase its concentration led to a further reprecipitation of POMA. The molecular weight distribution for POMA in solution 3 could not be obtained because the undoped polymer was only partially soluble in NMP, thus impairing the SEC analysis that was carried out for solution 1.

The experimental procedures for film fabrication are essentially the same as those described by Decher et al.[20] For the building of multilayers, POMA was alternated with PVS, where the latter was diluted in ultrapure water, with 82 μL of a 20 wt % aqueous solution of PVS (Aldrich) being mixed with 20 mL of water. The final PVS solution was completely clear. The rinsing solution was water with its pH adjusted to 3 with 1 M HCl. Films were adsorbed on BK7 optical glass (36 × 14 × 1 mm) that was rendered hydrophilic in a mixture of 30% hydrogen peroxide (H_2O_2)/concentrated sulfuric acid (H_2SO_4) in a 3:7 proportion. The slides were then rinsed with pure water and then further cleaned in a solution containing ultrapure water, H_2O_2, and ammonium hydroxide (NH_4OH) in a ratio of 5:1:1 by volume. BK7 glass was chosen because of its negligible absorbance in the visible region and its nicely polished surface. The POMA adsorption was monitored by measuring the UV−vis spectra with a double-beam Hitachi U2001 spectrophotometer.

Surface morphology was investigated using a Nanoscope IIIa (Digital Instruments) atomic force microscope (AFM) with 512 × 512 pixel images being obtained under ambient conditions in the tapping mode. The rms roughness, *W*, and the average height and average diameter of the aggregates were determined using the software from Digital Instruments. For scanning electron microscopy, a ZEISS-DSM960 system coupled to a Link QX 2000 was used.

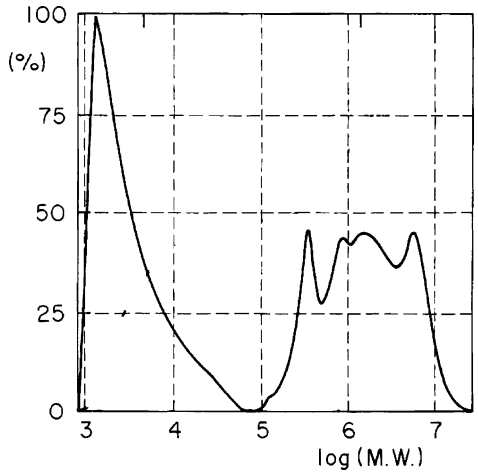

Figure 1. Molecular weight distribution of POMA sample obtained from solution 1.

III. Results and Discussion

The molecular weight distribution of the POMA sample obtained from solution 1 is shown in Figure 1. The distribution is completely inside the calibration curve exclusion limits.

The presence of at least two distinct regions of molecular weights is clearly visible. The mean molecular weights obtained for the first region were $M_w = 2.8 \times 10^6$ and $M_n = 8.5 \times 10^5$, and for the second region they were $M_w = 5.2 \times 10^3$ and $M_n = 2.3 \times 10^3$. The mean molecular weights calculated for the whole sample were $M_w = 1.4 \times 10^6$ and $M_n = 4.8 \times 10^3$, leading to an unusually high dispersity. We cannot prove unequivocally that the peaks that appear in the higher-molecular-weight region correspond only to longer chains and not to aggregates, as the sample hydrodynamic volume is compared with that of polystyrene standards, which do not exhibit the same behavior as POMA in solution. However, the conditions of molecular weight analysis (undoped sample, strong solvent, temperature, and high dilution) are less favorable to the formation of aggregates**.** As was stated in the Experimental Details section, the SEC analysis of the fractionated sample (solution 2) was not reliable because of its lower solubility in the solvent used in the chromatographic analysis. Assuming that the separation procedure does not induce chemical reactions in POMA molecules, this lower solubility can be seen as an indication that solution 3 is a higher-molecular-weight fraction than the POMA in solution 1. Therefore, solutions 1 and 3 used to fabricate the LBL films can be seen, in a first approximation, as comprising a highly polydisperse POMA sample and a less polydisperse sample with a high molecular weight. This conclusion is corroborated by the AFM data to be presented later.

The adsorption process of a polymer layer is affected by the substrate, and a uniform amount of POMA is adsorbed in each deposition process only after 5 or 6 POMA/PVS bilayers have been deposited.[21] We have therefore chosen to investigate the adsorption of the 11th or 16th POMA layer in the results to be presented. This ensures that substrate effects are no longer relevant. The time allowed for adsorption and the number of initially deposited layers are higher for the low-concentration solutions so that the films compared could have roughly the same UV−vis absorption (i.e., roughly the same thickness). The

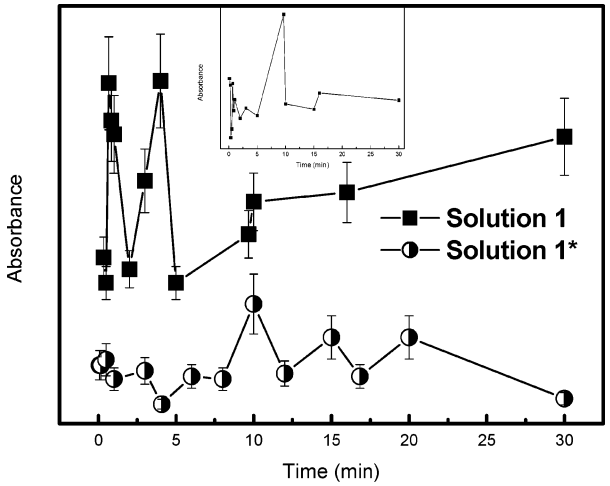

Figure 2. Film adsorption as a function of time of adsorption for the 11th POMA layer in a POMA/PVS LBL film obtained using solutions 1 and 1*. The inset shows the data for the 16th POMA layer in a POMA/PVS LBL film obtained using solution 1, which indicates that nonmonotonic behavior is also observed for this layer. No scale is given for the absorbance as the plots were shifted to facilitate visualization.

morphology was investigated for films obtained from the different POMA solutions. POMA/PVS films with 10 bilayers produced from solutions 1, 1*, and 3 display similar UV−vis absorption spectra but with a red shift for the film from the more concentrated[14] solution 1.

Polydisperse POMA (Solutions 1 and 1*). The kinetics of adsorption of POMA layers was found by Raposo et al.[21] to comprise two processes: an initial, fast process characteristic of a first-order kinetics that is due to nucleation of POMA domains and a second process corresponding to the growth of the domains that can be explained using a Johnson−Mehl−Avrami (JMA) function. In those results,[21] the amount of adsorbed material increased monotonically with time, as typically occurs for LBL films. However, for the highly polydisperse POMA, such a behavior was not observed. Figure 2 shows that the amount of POMA adsorbed increases nonmonotonically with time, for both high- (solution 1) and low-concentration (solution 1*) solutions. This suggests a competition between the adsorption and desorption processes. The error bars included in the figure are based on average values obtained for several samples fabricated under identical conditions. The dispersion is large, but does not jeopardize the conclusions drawn in the paper, as the nonmonotonic increase in the amount adsorbed can be inferred despite the dispersion. Note that the kinetic curves correspond to a true kinetics with one distinct film being used for each time of adsorption. If one single film were used for obtaining the curve, the repeated immersions would affect the amount of adsorbed material. In such cases, the increase in absorbance is monotonic with time (results not shown).

The competition is also manifested in the morphological properties of the POMA/PVS LBL films. Figure 3 shows a sequence of AFM images for POMA/PVS films prepared with solution 1. The images correspond to a POMA layer deposited on 10 bilayers of POMA/PVS, where each layer was adsorbed for 3 min. The time period for adsorption of the 11th POMA layer (top one) varied from 10 s to 12 h, and the scanning window for each image was 500 × 500 nm.

A globular structure was observed, similar to that reported for polyaniline films obtained with other techniques.[22] That the globular structure was not an experimental artifact induced by the AFM tip was confirmed by scanning electron microscopy, which should be exempt from such artifacts if they existed. The SEM results (provided as Supporting Information) did indicate a globular structure, with the same shape as in the AFM images. Note that, in Figure 3, the size of the grains increased and decreased as the time of adsorption increased, which is a surprising effect as one would expect the globules to increase monotonically with time until eventually reaching saturation. Therefore, the behavior is different from that observed by Raposo et al.[21] It should be stressed that the images in Figure 3 represent film morphology for already-formed surfaces as the AFM measurements were taken ex situ, with dried films. The roughness and thickness depend on the drying procedure, but the granular morphology is maintained.[23]

The rms roughness, W, after an initial jump increases slowly with the dimension of the scanning window, L, as shown in Figure 4. Although the dispersion obtained in experiments for different samples is high, the curve of Figure 4 represents the general behavior. Figure 5 shows that the rms roughness, W, exhibits an unusual nonmonotonic increase with time. As we discuss later, we cannot employ any scaling model to interpret these data, which would require W to reach saturation for a given L or time,[24] as this does not happen even for $L = 10\ \mu$m (see Figure 4).

Figure 6 shows that the average diameter of the globules increases practically linearly with their average height for different periods of time, thus demonstrating that there is no preferential direction for the growth of the globules (note that the data in Figure 6 were obtained from samples that had about the same rms roughness). There are multiple data points for some times of adsorption because measurements were taken at distinct places on the sample. In a previous work,[16] using AFM data and applying the JMA equation to the adsorption kinetics, we concluded that the aggregates grow symmetrically, as shown in Figure 6. The Avrami parameter then found ($n = 4$) indicates that the aggregates grow sporadically via a diffusion-controlled mechanism and with a nucleation rate that increases with time. That is, new nuclei are created in regions where polymer is already adsorbed, which means that POMA adsorbs over POMA.

The results presented here are similar to the oscillation with time for the adsorption of protonated poly(2-vinylpyridine) (PVP) on silica particles.[25] This behavior was attributed to a cooperative adsorption process comprising several subsequent adsorption−desorption steps. In the adsorption experiments with POMA/PVS films, POMA molecules and water molecules compete for adsorption. When highly polydisperse POMA is used, the charge density varies depending on the molecule size. As the substrate is immersed into the POMA solution, the molecules close to the surface will adsorb, regardless of their size. As time evolves, smaller molecules have higher probability of adsorbing as they take less time to diffuse through the solution and reach the substrate. If the substrate remains immersed, however, larger molecules with higher charge densities will eventually reach the substrate and possibly replace the smaller molecules.[26] This rationale is similar to that suggested by Schoeler et al.,[27] who investigated the adsorption characteristics of polymers with variable degrees of charge. In their work, a weakly charged copolymer was desorbed when the film was immersed into a solution of a highly charged polyelectrolyte of opposite charge. Therefore, the weakly charged copolymer was only weakly adsorbed, which led to an adsorption/desorption competition.[27] Another factor that can lead to adsorption/desorption is the competition between ionic forces and secondary interactions (such as H-bonding) for adsorption. For instance,

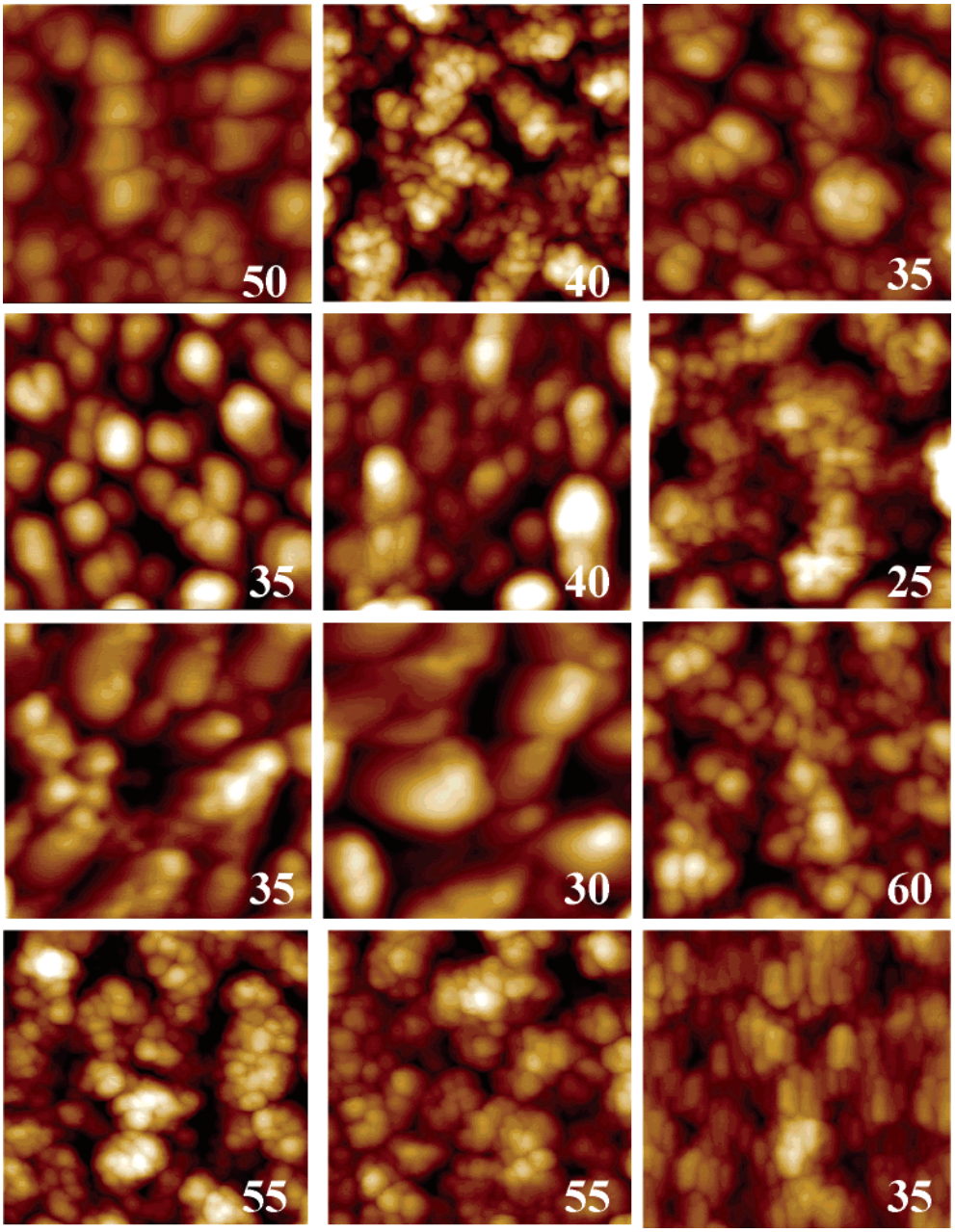

Figure 3. AFM images of LBL films with a POMA layer adsorbed on top of 10 bilayers of POMA/PVS, obtained using solution 1. The time periods of adsorption for the 11th layer were 0, 10, 30 s; 1, 2, 10, 15, 30 min; 1, 2, 3, and 12 h (starting from the top left corner and moving to the right and down). The scanned length was $L = 500$ nm. The number annotated in each image refers to the surface height (z axis).

Clark and Hammond[28] exploited such competition to dramatically change the affinity of a polymer for the surface on LBL films.

Treated POMA Solution (Solution 3). Figure 7 shows that the kinetics of adsorption for POMA layers adsorbed from solution 3 displays the usual monotonic increase in the adsorbed amount with time. This curve can also be interpreted as comprising a two-step process, in which the first step is represented by a first-order kinetics with a characteristic time of approximately 20 s. The second process can be explained with a Johnson−Mehl−Avrami (JMA) function (eq 1) with n between 1 and 1.5 and characteristic times of hundreds of seconds (~600 s), with the time being close to the value reported by Raposo et al.[21] To choose the most appropriate value of n, we resort to the morphological characterization of POMA LBL films that showed a columnar growth of aggregates[14] consistent with $n = 1$. The solid line in Figure 7 was then obtained with eq 1 with $n = 1$

$$A = k_1\left[1 - \exp\left(-\frac{t}{\tau_1}\right)\right] + k_2\left\{1 - \exp\left[-\left(\frac{t}{\tau_2}\right)^n\right]\right\} \quad (1)$$

where A is the absorbance; k_1, k_2, and n are constants; and τ_1 and τ_2 are the characteristic times.

The AFM images of POMA/PVS LBL films obtained from the treated POMA solution, with a concentration of 0.03 g/L (solution 3), are shown in Figure 8, where all POMA layers were adsorbed for 30 min. By comparing the image in Figure 8 for 30 min and $L = 500$ nm with the corresponding image in Figure 3, we note that, in contrast to the films obtained from solution 1, the size of the granules is much more uniform and the coverage of the bK7 glass is also better for the films obtained

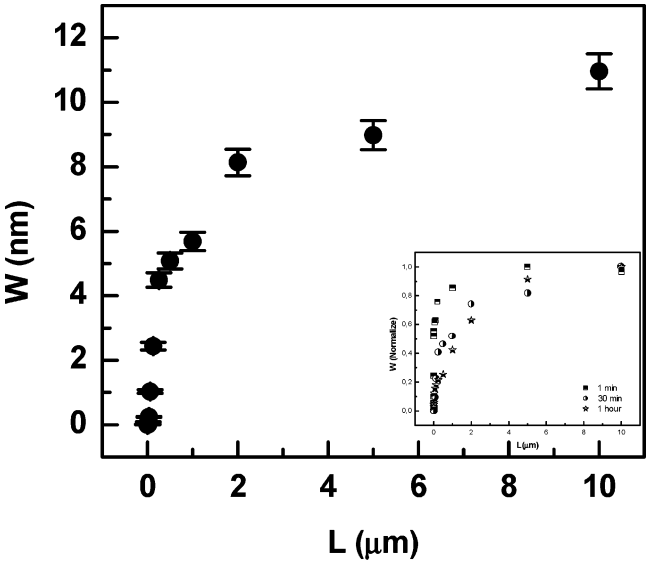

Figure 4. rms roughness versus size of the scanning window for the 11th POMA layer adsorbed for 30 min from the polydisperse POMA solution 1.

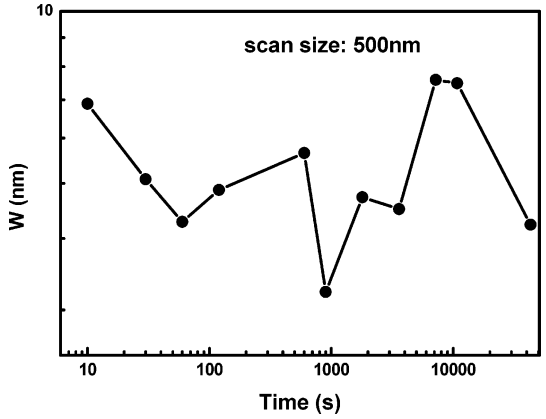

Figure 5. log *W* versus log time plot in the scan size of 500 nm for POMA/PVS LBL films obtained from solution 1.

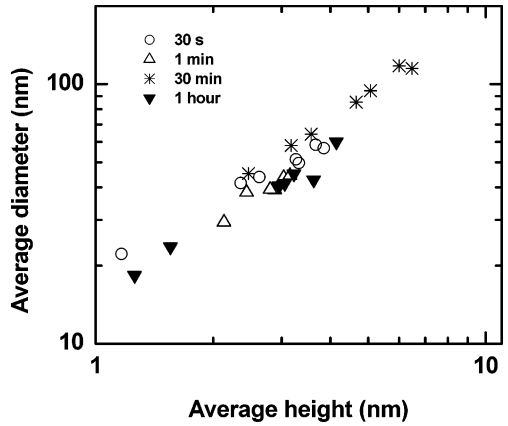

Figure 6. Average diameter versus average height of the globules for the 11th POMA layer (solution 1) adsorbed for various periods of time with a scanning window length $L = 1$ μm.

from solution 3. The better uniformity in the granule size indicates that the fractionation process leading to solution 3 was reasonably efficient.

Figure 9 shows that, for low concentration of the treated POMA, *W* increases slowly with *L*, with roughness varying from 1.8 to 5 nm. The error bars were obtained by taking averages

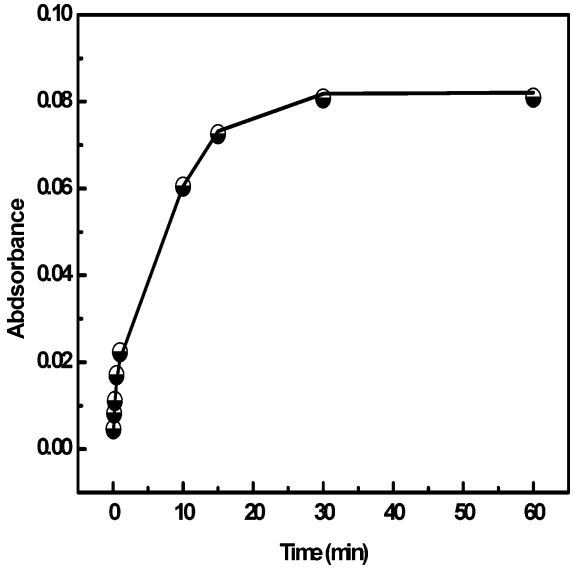

Figure 7. Film absorption as a function of time of adsorption for the 16th POMA layer on a POMA/PVS LBL film obtained using solution 3. The solid line represents the fitting using eq 1.

of several images obtained under identical conditions, i.e., with samples prepared under identical conditions.

It is now possible to apply scaling laws as *W* saturates at a given *L*, which allows one to investigate the morphology and dynamics of film growth. The parameters involved are the roughness; the fractal dimension; and the critical exponents, namely, the exponent of roughness (α), the exponent of growth (β), and the dynamic exponent (z). Scaling laws therefore help describe how film morphology, characterized by rms roughness, evolves during film growth, based on two factors: the time of formation of the surface and the size of the scanning window. The rms roughness *W* is taken as a function of the scanning window size, *L*, in the form $W(L) \propto L^{\alpha}$, where α is independent of the units employed for the lateral dimension *L*. α should be calculated when the roughness value has already reached saturation, as in Figure 9. The inset of the figure displays the log *W* vs log *L* plot, where a linear region can be seen, i.e., the scaling law is obeyed, leading to $\alpha = 0.8 \pm 0.1$. This value is consistent with those reported in the literature, falling in the range $0.7 < \alpha < 0.9$.[4,29−32] α is related to the fractal dimension (DF) by[32] DF $= D - \alpha(t)$, where *D* is the dimension of the space associated with the growth. A value of $\alpha < 1$ is characteristic of a fractal self-affine surface formation,[33] where the fractal dimension can be estimated as DF $= 3 - \alpha$. For our films, the fractal dimension is ca. 2.2 ± 0.1 (DF $= 2 \Rightarrow$ planar surface).[33] There is no comprehensive theory to explain or predict α for a complex system such as an adsorbed polymer film,[32] particularly because morphological properties can depend on the preparation conditions, as illustrated here. Results reported recently by Lobo et al.[13] also support these conclusions. Observing the variation of α with the number of layers of POMA/PVS deposited and with the type of substrate used[13] indicates that the changes in the fractal dimensions were not systematic and that single model growth models cannot explain this behavior.

The films obtained from solution 3 are less rough than the POMA/PVS films prepared with higher POMA concentrations (0.2 g/L),[35] but they are rougher than an LBL film adsorbed from solution 1* (see below) that is less concentrated. This indicates that the roughness increases with the solution concentration. When the concentration is approximately the same, as in the case of solutions 1* and 3, the film produced—under

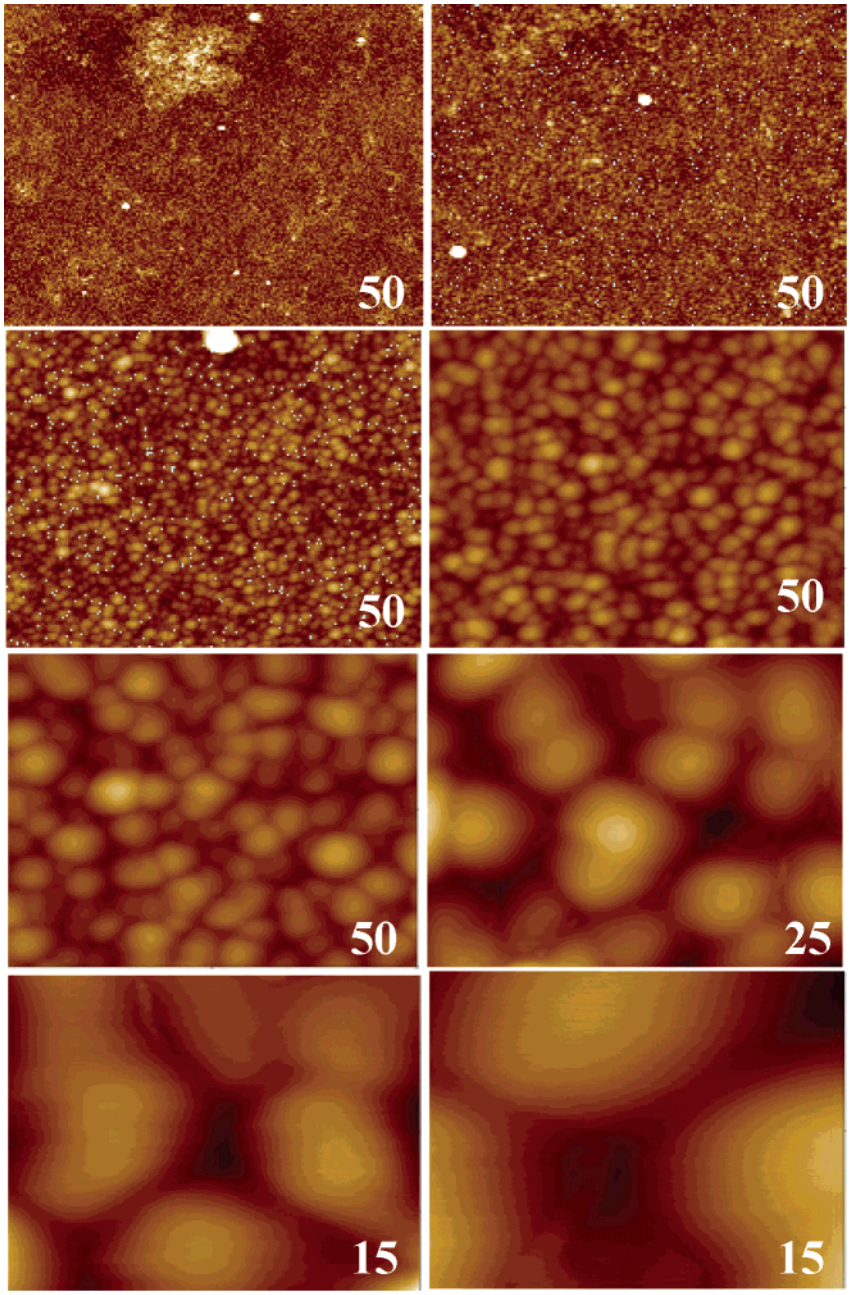

Figure 8. AFM images of a 16-bilayer POMA/PVS film where all layers were adsorbed for 30 min, using POMA solution 3. The scanning window size was $L = 10$, 5, 2, and 1 μm; 500, 200, 100, and 50 nm (starting from the top left corner and moving to the right and down). The number annotated in each image refers to the surface height (z axis).

identical conditions—from the POMA fraction with higher molecular weight displays larger roughness as well as larger granules. This can be seen in Figure 10, where the rms roughnesses are 2 and 5 nm for LBL films from solutions 1* and 3, respectively.

Figure 11 shows that the average height of the granules decreases with their diameter for the 16-bilayer POMA/PVS films from solution 3 where all POMA layers were adsorbed for 30 min. That is, there is preferential growth in the vertical direction, unlike the films prepared with the highly polydisperse POMA from solution 1 (Figure 6), for which no preferential direction for growth was observed.

IV. Conclusions

In this paper, we showed that the adsorption and morphological properties of LBL films depend on the treatments the polymer undergoes prior to the adsorption process. For the specific case of POMA, precipitation from a strong acidic solution probably leads to a less polydisperse sample that yields remarkably distinct results for the LBL films when compared to a highly polydisperse material. The dimension of the globular structures seen by AFM increases nonmonotonically during film growth for the polydisperse POMA, owing to adsorption/desorption competition. The treated POMA had lower solubility probably as a consequence of a higher molecular weight, which caused the granules to be larger than for films obtained from the polydisperse POMA. A lower dispersity is manifested by a more homogeneous distribution of globule sizes in the LBL films, whose kinetics of adsorption could be explained with a two-step process. The morphological properties of the LBL films from treated POMA could also be interpreted using a scaling law with a fractal dimension of 2.2, close to that found for

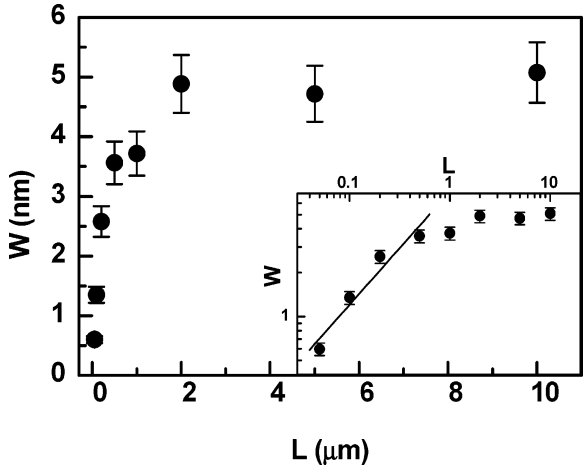

Figure 9. rms roughness versus scan size for the 16th POMA layer adsorbed for 30 min using POMA solution 3 and corresponding to the data obtained from the images of Figure 8. The inset shows the log W versus log L plot for L in the range from 0.05 to 10.

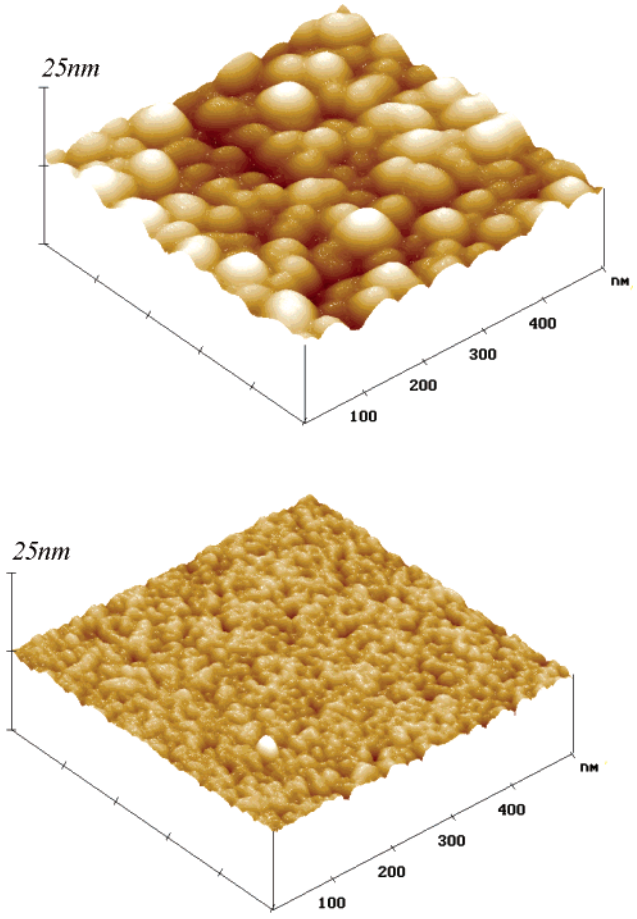

Figure 10. AFM image of a 16-bilayer POMA/PVS LBL film obtained with solutions 1* (bottom image) and 3 (top image). The globules in the AFM image for solution 3 are larger than those in the image for solution 1*.

chemical vapor deposited (CVD) silicon and electrodeposited copper on gold. The similarity was not expected but shows that, for this particular solution, regardless of the technique used to grow the film, the DF values are similar and lead to structures as flat as those obtained by other techniques. A step further in this investigation consists of varying the polydispersity and concentration systematically to find the critical values below which more homogeneous films can be obtained.

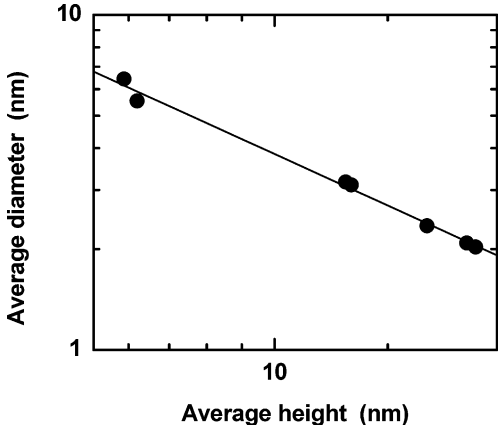

Figure 11. Mean diameter versus average height of the granules in a 16-bilayer POMA/PVS film obtained using POMA solution 3. $L = 1$ μm (from data in Figure 8).

Acknowledgment. The authors acknowledge the financial assistance of FAPESP and CNPq (Brazil).

Supporting Information Available: SEM images of a POMA layer deposited on 10 bilayers of POMA/PVS, confirming the globular structure detected by AFM. This material is available free of charge via the Internet at http://pubs.acs.org.

References and Notes

(1) Ferreira, M.; Rubner, M. F. *Macromolecules* **1995**, *28*, 7107.
(2) Petty, M. C. *Langmuir−Blodgett Films*; Cambridge University Press: Cambridge, U.K., 1996.
(3) Pontes, R. S.; Raposo, M.; Camilo, C. S.; Dhanabalan, A.; Ferreira, M.; Oliveira, O. N., Jr. *Phys. Status Solidi A* **1999**, *173*, 41.
(4) Ojeda, F.; Cuervo, R.; Salvarezza, R.; Vázquez, L. *J. Phys. IV Fr.* **1999**, *9*, 265.
(5) Oliveira, O. N., Jr.; He, J.-A.; Zucolotto, V.; Balasubramanian, S.; Li, L.; Nalwa, H. S.; Kumar, J.; Tripathy, S. K. In *Handbook of Polyelectrolytes*; Tripathy, S. K., Kumar, J., Nalwa, H. S., Eds.; American Scientific Publishers: Los Angeles, 2002; Vol. 1 Layer-by-Layer Polyelectrolyte Films for Electronic and Photonic Applications, pp 1−37.
(6) Park, S. Y.; Barrett, C. J.; Rubner, M. F.; Mayes, A. M. *Macromolecules* **2001**, *34*, 3384.
(7) Anzai, J.; Kobayashi, Y.; Nakamura, N.; Nishimura, M.; Hoshi, T. *Langmuir* **1999**, *15*, 221.
(8) Macdiarmid, A. G.; Chiang, J. C.; Richter, A. F.; Epstein, A. J. *Synth. Met.* **1987**, *18*, 285.
(9) Stafström, S.; Brédas, J. L.; Epstein, A. J.; Woo, H. S.; Tanner, D. B.; Huang, W. S.; MacDiarmid, A. G. *Phys Rev. Lett.* **1987**, *59*, 1464.
(10) Mattoso, L. H. C.; Patterno, L. G.; Campana, S. P.; Oliveira, O. N., Jr. *Synth. Met.* **1997**, *84*, 123.
(11) Raposo M.; Oliveira, O. N., Jr. *Langmuir* **2000**, *16*, 2839.
(12) Raposo, M.; Oliveira, O. N., Jr. *Langmuir* **2002**, *18*, 6874.
(13) Lobo, R. F. M.; Pereira-da-Silva, M. A.; Raposo, M.; Faria, R. M.; Oliveira, O. N., Jr. *Nanotechnology* **2003**, *14*, 101.
(14) de Souza, N. C.; Silva, J. R.; Rodrigues, C. A.; Costa, L. D.; Giacometti, J. A.; Oliveira, O. N., Jr. *Thin Solid Films* **2003**, *428*, 232.
(15) Ram, M. K.; Salerno, M.; Adami, M.; Faraci, P.; Nicolini, C. *Langmuir* **1999**, *15*, 1252.
(16) de Souza, N. C.; Silva, J. R.; Rodrigues, C. A.; Hernandes, A. C.; Costa, L. D.; Giacometti, J. A.; Oliveira, O. N., Jr. *Synth. Met.* **2003**, *135*, 121.
(17) Ram, M. K.; Adami, M.; Sartore, M.; Salerno, M.; Paddeu, S.; Nicolini, C. *Synth. Met.* **1999**, *100*, 249.
(18) Marletta, A., Piovesan, E.; Dantas, N. O.; de Souza, N. C.; Olivati, C. A.; Balogh, D. T.; Faria, R. M.; Oliveira, O. N., Jr. *J. Appl. Phys.* **2003**, *94*, 5592.
(19) Mattoso, L. H. C.; Faria, R. M.; Bulhões, L. O. S.; MacDiarmid, A. G. *J. Polym. Sci. A: Polym. Chem.* **1994**, *32*, 2147.
(20) Decher, G.; Hong, J. D.; Schmitt, J. *Thin Solid Films* **1992**, *210/211*, 831.
(21) Raposo, M.; Pontes, R. S.; Mattoso, L. H. C.; Oliveira, O. N., Jr. *Macromolecules* **1997**, *30*, 6095.
(22) Porter, T. L *Surf. Sci.* **1993**, *293*, 81.
(23) Costa, L. D.; Rodrigues, C. A.; De Souza, N. C.; Oliveira, O. N., Jr. *J. Nanosci. Nanotechnol.* **2003**, *3*, 257.

(24) Barabási A. L.; Stanley H. E. *Fractal Concepts in Surface Growth*; Cambridge University Press: New York, 1995.
(25) Minko, S.; Voronov, A.; Pefferkon, E. *Langmuir* **2000**, *16* (20), 7876.
(26) Sukhishvili, S. A.; Granick, S. *J. Chem. Phys.* **1998**, *109* (16), 6869.
(27) Schoeler, B.; Kumaraswamy, G.; Caruso, F. *Macromolecules* **2002**, *35*, 889.
(28) Clark, S. L.; Hammond, P. T. *Langmuir* **2000**, *16* (26), 10206.
(29) Vela, M. E.; Andreasen, G.; Salvarezza, C.; Arvia, A. J. *J. Chem. Soc., Faraday Trans*. **1996**, *92* (20), 4093.
(30) Schmidt, W. U.; Alkire, R. C.; Gerwirth, A. A. *J. Electrochem. Soc.* **1996**, *143*, 3122.
(31) Salvarezza, R. C.; Vázquez, L.; Herrasti, P.; Ocón, P.; Vara, J.; Arvia, A. J. *Europhys. Lett*. **1992**, *20* (8), 727.
(32) Vázquez, L.; Salvarezza, R. C.; Herrasti, P.; Ocón, P.; Vara, J.; Arvia, A. J. *Appl. Surf. Sci.* **1993**, *70/71*, 413.
(33) Yoshinobu, T.; Iwamoto, A.; Iwasaki, H. *Jpn. J. Appl. Phys*. **1994**, *33*, L67.
(34) Almqvist, N. *Surf. Sci.* **1996**, *355*, 221.
(35) Raposo, M.; Lobo, R. F. M.; Pereira-Da-Silva, M. A.; Faria, R. M.; Oliveira, O. N., Jr. Thickness and roughness measurements in poly-(*o*-methoxyaniline) layer-by-layer films using AFM. In *Proceedings of the International Symposium on Electrets, 10, Delphi, 1999*; IEEE Press: Piscataway, NJ, 1999; pp 533−535.